



Unusually Low Heat of Adsorption of CO₂ on AIPO and SAPO Molecular Sieves

Eduardo Pérez-Botella^{1*}, Raquel Martínez-Franco², Nuria González-Camuñas¹, Ángel Cantín¹, Miguel Palomino¹, Manuel Moliner¹, Susana Valencia¹ and Fernando Rey¹

¹ Instituto de Tecnología Química, Universitat Politècnica de València-Consejo Superior de Investigaciones Científicas, Valencia, Spain, ² Institut Français du Pétrole (IFP) Energies Nouvelles, Lyon, France

OPEN ACCESS

Edited by:

Enrique Rodríguez-Castellón,
University of Malaga, Spain

Reviewed by:

Carlos Adolfo Grande,
SINTEF Industry, Norway
Jotheeswari Kothandaraman,
Pacific Northwest National Laboratory
(DOE), United States

*Correspondence:

Eduardo Pérez-Botella
edpebo@upvnet.upv.es

Specialty section:

This article was submitted to
Green and Sustainable Chemistry,
a section of the journal
Frontiers in Chemistry

Received: 29 July 2020

Accepted: 18 September 2020

Published: 28 October 2020

Citation:

Pérez-Botella E, Martínez-Franco R,
González-Camuñas N, Cantín Á,
Palomino M, Moliner M, Valencia S
and Rey F (2020) Unusually Low Heat
of Adsorption of CO₂ on AIPO and
SAPO Molecular Sieves.
Front. Chem. 8:588712.
doi: 10.3389/fchem.2020.588712

The capture of CO₂ from post-combustion streams or from other mixtures, such as natural gas, is an effective way of reducing CO₂ emissions, which contribute to the greenhouse effect in the atmosphere. One of the developing technologies for this purpose is physisorption on selective solid adsorbents. The ideal adsorbents are selective toward CO₂, have a large adsorption capacity at atmospheric pressure and are easily regenerated, resulting in high working capacity. Therefore, adsorbents combining molecular sieving properties and low heats of adsorption of CO₂ are of clear interest as they will provide high selectivities and regenerabilities in CO₂ separation process. Here we report that some aluminophosphate (AIPO) and silicoaluminophosphate (SAPO) materials with LTA, CHA and AFI structures present lower heats of adsorption of CO₂ (13–25 kJ/mol) than their structurally analogous zeolites at comparable framework charges. In some cases, their heats of adsorption are even lower than those of pure silica composition (20–25 kJ/mol). This could mean a great improvement in the regeneration process compared to the most frequently used zeolitic adsorbents for this application while maintaining most of their adsorption capacity, if materials with the right stability and pore size and topology are found.

Keywords: carbon dioxide, separation, adsorption, capture, molecular sieves, zeolites

INTRODUCTION

Carbon dioxide is a greenhouse gas that is emitted to the atmosphere due to a large number of industrial processes. Combustion of fossil fuels for transport or in power plants, metallurgy, cement and chemical production are some of the most important processes related to CO₂ massive release to the atmosphere (U.S. National Coal Council, 2015). In order to mitigate CO₂ emissions and prevent the negative effect they have on climate change, Carbon Capture and Storage (CCS) technologies are being applied and developed. CCS from air is the only way of reducing CO₂ presence in the atmosphere, while CCS from large point sources (i.e., power plant or cement factory exhaust) is the best way of minimizing future emissions (Boot-Handford et al., 2014; Leung et al., 2014; The National Academies of Sciences, Engineering and Medicine, 2018).

The currently most common technology for CCS from large point sources is amine scrubbing, which involves flowing the CO₂-containing mixture through a liquid solution of amines and its thermal regeneration afterwards. This is a highly energy demanding process, which as well presents problems with reactant stability and corrosion of the equipment. Thus, along with optimization

of this technology in what refers to heat integration and reactant improvement, a number of alternative methods is being researched and developed, such as oxycombustion or separation using either membranes or adsorbents (Boot-Handford et al., 2014; Rubin et al., 2015; Bui et al., 2018; Global CCS Institute, 2019).

Separation by adsorption is being researched, as its operation costs have potential to be lower than those of other current processes. Materials that have been studied as adsorbents for CO₂ include carbonaceous materials, metal-organic frameworks (MOFs), covalent organic frameworks (COFs), supported amines, zeolites, AlPOs, and SAPOs (Lee et al., 2008; Tagliabue et al., 2009; Liu et al., 2011; Cheung et al., 2012; Lee and Park, 2015; Fischer, 2017; Riboldi and Bolland, 2017). Selectivity, working capacity and easiness of regeneration are the three parameters to be maximized in the selection of an adsorbent. Out of the mentioned materials, supported amines and some MOFs and low silica zeolites interact chemically with CO₂, i.e., chemisorption takes place. The CO₂/CH₄ and CO₂/N₂ selectivities on these materials is usually very high, due to the specific interaction between the CO₂ and the adsorbent. However, this strong interaction also leads to large amounts of energy required for regeneration. These kinds of adsorbents are usually hydrophilic (or even water-sensitive) too, which is another major drawback, as water and CO₂ adsorption interfere with each other.

Adsorption of CO₂ on high and pure silica zeolites, together with carbonaceous materials, many MOFs and AlPOs and SAPOs takes place via a physisorption mechanism, which means that the interaction between sorbent and sorbate is weaker, thus meaning regeneration will be less energy intensive. Nevertheless, this does not mean that CO₂/CH₄ and/or CO₂/N₂ selectivities have to be low. Compositional and structural tuning of carbonaceous materials, MOFs (Lee and Park, 2015), zeolites, AlPOs, and SAPOs (García et al., 2014; Fischer, 2017) can lead to materials with high selectivities, capacities and low regeneration energies.

AlPOs and SAPOs are microporous materials closely related to zeolites and present a framework based on alternating PO₄ and AlO₄ tetrahedra. In the case of SAPOs, some P atoms can be replaced by isolated Si atoms and pure silica domains (Si-rich domains or Si-islands) can also be present (Man et al., 1991). These materials were discovered in the early 1980s (Wilson et al., 1982; Lok et al., 1984). Since then, AlPOs and SAPOs with many different structures have been prepared and studied as catalysts or adsorbents (Zibrowius et al., 1992; Martin et al., 1998; Schreyeck et al., 1998; Wright and Connor, 2008; Liu et al., 2011; Cheung et al., 2012; Martínez-Franco et al., 2015; Dawson et al., 2017; Fischer, 2017).

In this work, we have studied the adsorption of CO₂ on AlPOs and SAPOs with LTA, CHA, and AFI structures (Baerlocher and McCusker), and compared the calculated isosteric heats of adsorption with those of analogous zeolites previously reported. The choice of adsorbent structures was made in order to include

TABLE 1 | Framework composition as determined per ICP, isolated Si fraction as determined from ²⁹Si-NMR spectra and the estimated framework negative charge.

Sample	X _{Si}	X _{Al}	X _P	Isolated Si fraction, from NMR	Estimated framework negative charge
AlPO-42	–	0.53	0.47	–	0
SAPO-42-104	0.04	0.50	0.46	0.24	0.010
SAPO-42-24	0.05	0.52	0.43	0.82	0.041
SAPO-42-13	0.1	0.54	0.36	0.8	0.080
Si-LTA	1	–	–	–	0
LTA-31	0.97	0.03	–	–	0.032
LTA-6	0.83	0.17	–	–	0.167
LTA-4.5	0.78	0.22	–	–	0.222
LTA-3	0.67	0.33	–	–	0.333
AlPO-34	–	0.57	0.43	–	0
SAPO-34-10	0.10	0.55	0.35	0.975	0.097
SAPO-34-7	0.18	0.51	0.31	0.814	0.146
Si-CHA	1	–	–	–	0
CHA-19	0.95	0.05	–	–	0.052
CHA-18	0.94	0.06	–	–	0.055
CHA-6	0.84	0.16	–	–	0.164
CHA-3	0.65	0.35	–	–	0.348
AlPO-5	–	0.54	0.46	–	0
SAPO-5-46	0.04	0.53	0.43	0.6	0.022
SAPO-5-34	0.07	0.54	0.40	0.45	0.030
Si-AFI	1	–	–	–	0

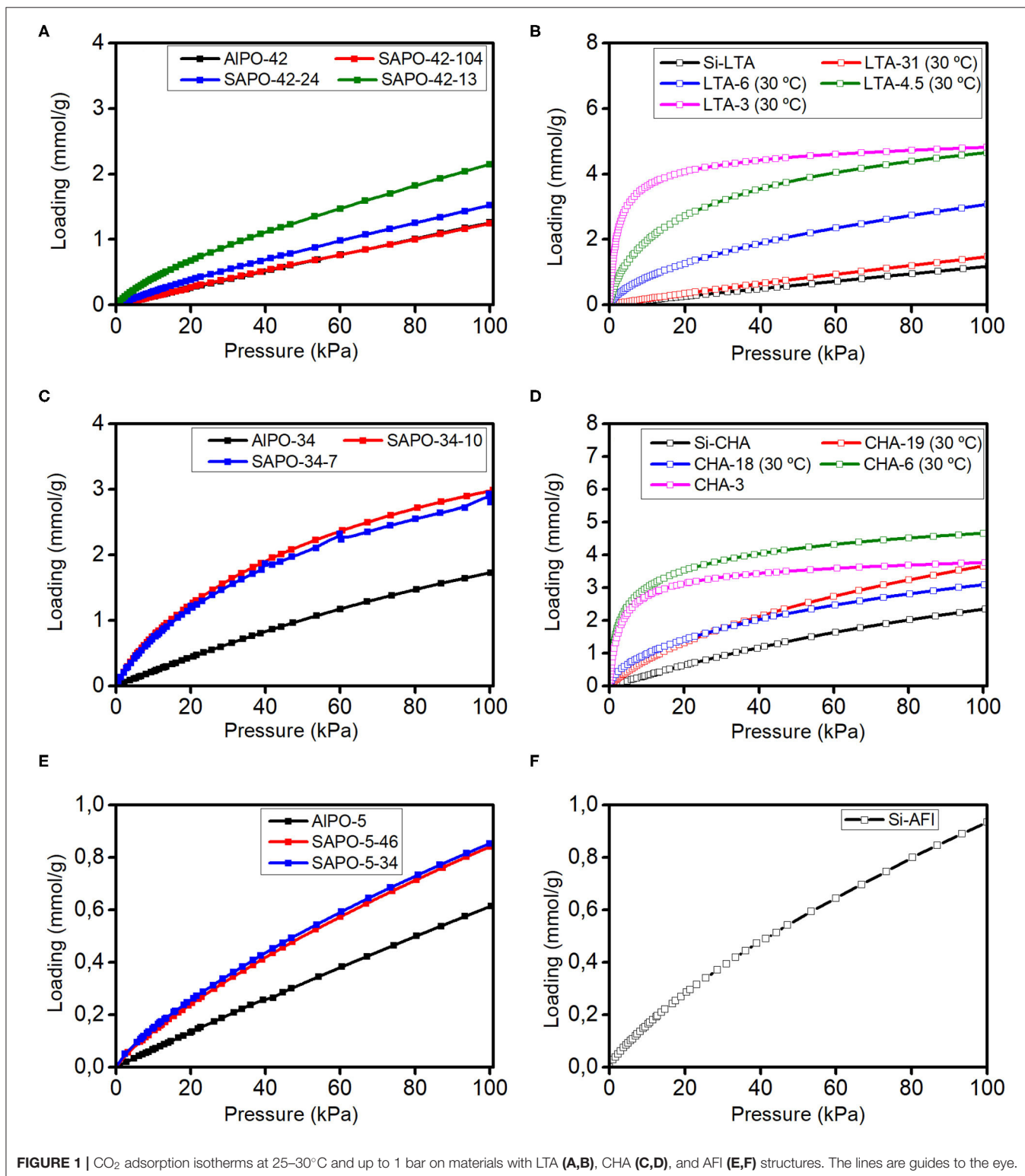
TABLE 2 | Textural properties of the studied adsorbents.

Sample	BET surface area (m ² /g)	Micropore volume (cm ³ /g)	DA surface area (m ² /g)
AlPO-42	774	0.290	–
SAPO-42-104	797	0.301	–
SAPO-42-24	776	0.289	–
SAPO-42-13	743	0.275	–
Si-LTA	811	0.320	–
LTA-31	777	0.305	–
LTA-6	806	0.297	–
LTA-4.5	799	0.304	680
LTA-3	794	0.295	609
AlPO-34	–	0.226	–
SAPO-34-10	595	0.210	–
SAPO-34-7	699	0.242	–
Si-CHA	821	0.296	–
CHA-19	869	0.305	–
CHA-18	801	0.293	–
CHA-6	749	0.273	600
CHA-3*	–	–	470
AlPO-5	310	0.117	–
SAPO-5-46	383	0.141	–
SAPO-5-34	355	0.119	–
Si-AFI	359	0.130	–

*N₂ isotherms at 77 K could not be obtained due to very slow diffusion.

two small pore structures (LTA and CHA) which have been extensively reported as selective CO₂ adsorbents (Tagliabue et al., 2009; Palomino et al., 2010; Miyamoto et al., 2012; Shang et al., 2012; Pham et al., 2014). Materials with AFI structure were

included in order to check if the same findings obtained for small pore materials applied as well to large pore zeotypes. The surprisingly low isosteric heats of adsorption found in these materials suggest that AlPOs and SAPOs can present major



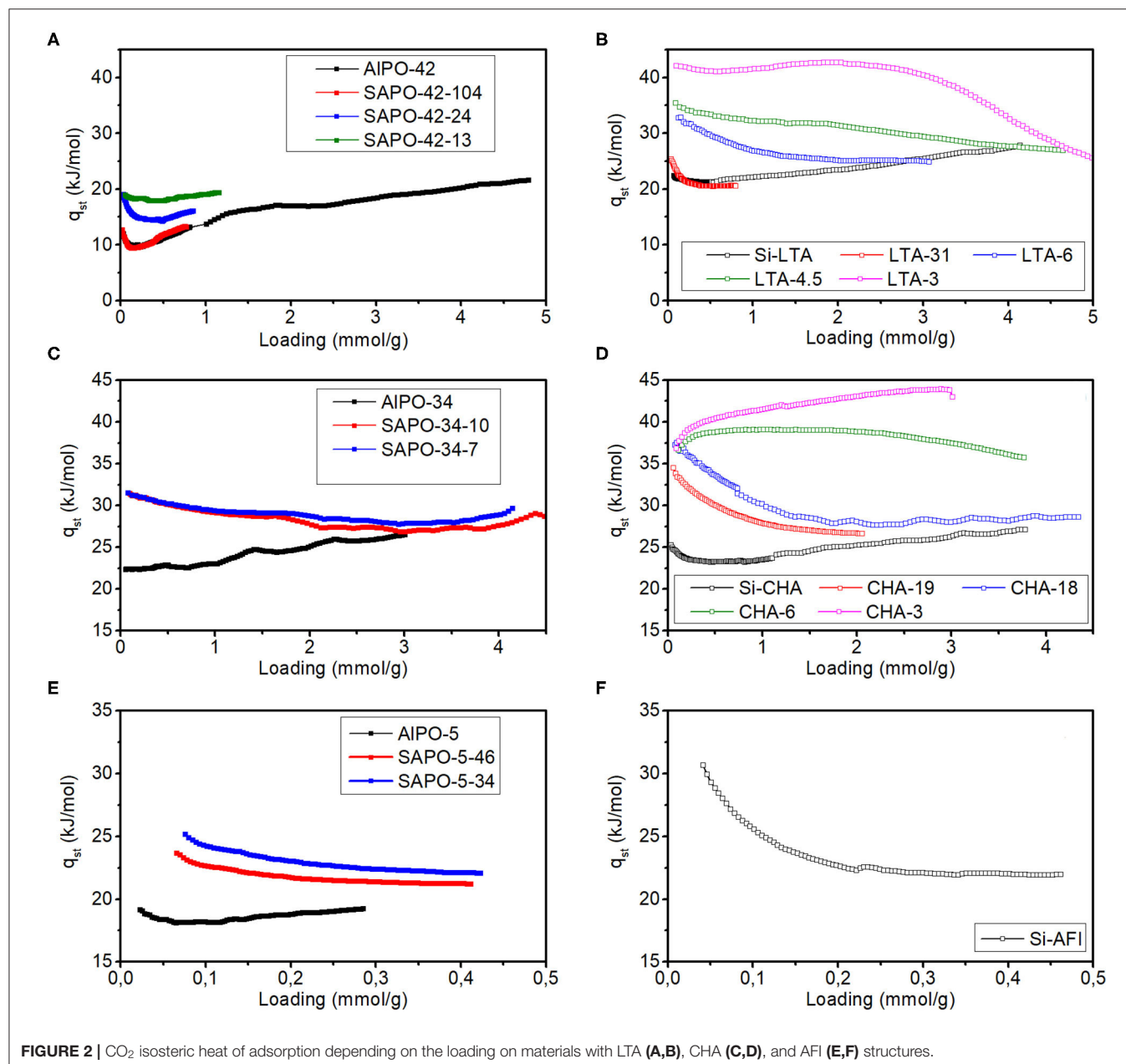
advantages in the field of CO₂ separation and adsorption in comparison to zeolites, if materials with structures that maximize selectivities over methane or nitrogen are found.

MATERIALS AND METHODS

Synthesis of Materials

Experimental details on the synthesis procedures used can be found in the **Supplementary Material**. The naming of the samples has been explained in the SM, as well. Zeolites with LTA structure and different aluminum content were prepared as reported in IZA, Kühn (1980), Moscoso et al. (2003), Corma et al. (2004), Palomino et al. (2010), and Lemishko et al.

(2016). AIPO-42, with LTA structure, was synthesized according to the method reported in Schreyeck et al. (1998) and SAPO-42 materials with different Si distribution were prepared as reported in Martínez-Franco et al. (2015). Pure silica CHA and CHA-19 were synthesized using a previously reported method (Díaz-Cabañas and Barrett, 1998). Other CHA zeolitic samples containing Al (CHA-3; CHA-18) were synthesized according to procedures reported on the Verified Syntheses of Zeolitic Materials of the International Zeolite Association (VSZM-IZA) (Bourgogne et al., 1985; Zones and van Nordstrand, 1988; IZA) and CHA-6 was synthesized according to Zones (1991). SAPO-34-10 was prepared following a recently described procedure using tetraethylammonium hydroxide (TEAOH) as the OSDA



(Martínez-Franco et al., 2016). SAPO-34-7 was also synthesized according to the procedure reported on the VSZM-IZA (Prakash and Unnikrishnan, 1994; IZA). Zeolite SSZ-24 (pure silica AFI) was synthesized according to a procedure reported on the VSZM-IZA (Nordstrand et al., 1988; IZA). AlPO-5 and SAPO-5 materials were synthesized following a procedure reported on the VSZM-IZA (Young and Davis, 1991; Girnus et al., 1995; IZA).

AlPO-34 was synthesized according to a novel method using (S)-1-methyl-2-(pyrrolidin-1-ylmethyl)pyrrolidine (Supplementary Figure 2) as the organic structure directing agent (OSDA). The OSDA was dispersed in a solution of phosphoric acid in water. Aluminum isopropoxide was then added and the resulting mixture stirred for 2 h at room temperature for homogenization. Hydrofluoric acid was then added, reaching pH = 7 and the resulting mixture was stirred for 1 h at room temperature. The resulting gel composition was:



The gel was introduced in a Teflon lined autoclave and kept at 175°C for 18 h with no stirring. The solid was recovered by filtration and after thorough washing with water, dried in an oven at 100°C. The resulting solid was calcined in air at 650°C.

Characterization

Structural characterization of the studied materials was performed by powder X-Ray Diffraction (XRD) using a CUBIX PANalytical diffractometer, operating with CuK α radiation ($\lambda_1 = 1.5406 \text{ \AA}$) at 45 kV and 40 mA in the 2θ range from 4 to 40°. Some samples were measured after dehydration by applying heat and under dry air flow using an *in situ* reaction chamber Anton-Paar XRK-900 attached to a PANalytical Empyrean diffractometer with CuK α radiation ($\lambda_1 = 1.5406 \text{ \AA}$) at 45 kV and 40 mA in the 2θ range from 3 to 75°.

The connectivity and chemical environment of the framework species were studied by magic angle spinning nuclear magnetic resonance (MAS NMR) spectroscopy at room temperature. A Bruker Avance III HD 400 MHz spectrometer was used for this purpose. ^{27}Al MAS NMR were recorded at $\nu_0(^{27}\text{Al}) = 104.21 \text{ MHz}$ at a spinning rate of 20 kHz with a 90° pulse length of 1.3 μs with a 1 s repetition time. The ^{27}Al chemical shift was referred to $\text{Al}(\text{NO}_3)_3 \cdot 9\text{H}_2\text{O}$. ^{31}P NMR spectra were recorded at $\nu_0(^{31}\text{P}) = 161.9 \text{ MHz}$ using spinning rate of 10 kHz, a 90° pulse length of 3.7 μs with spinal proton decoupling and a repetition time of 20 s. The ^{31}P chemical shift was referred to phosphoric acid. ^{29}Si NMR spectra were recorded at $\nu_0(^{29}\text{Si}) = 79.5 \text{ MHz}$ using a spinning rate of 5 kHz with a 60° pulse length of 3.5 μs , spinal proton decoupling and 180 s as repetition time. The ^{29}Si chemical shift was referred to tetramethylsilane.

The chemical composition of the solids was analyzed by inductively coupled plasma optical emission spectroscopy (ICP-OES) using a Varian 715-ES device.

Scanning electron microscopy (SEM) images were obtained using a Zeiss Ultra 55 microscope with an accelerating voltage of 1 kV.

The textural analysis was performed by measuring N_2 isotherms at 77 K on volumetric Micromeritics ASAP 2020 and

2420 devices after activation at 400°C and under vacuum. The Brunauer-Emmet-Teller (BET) and t-plot methods were used in order to obtain estimations of the surface area and the micropore volume, respectively (Thommes et al., 2015). In some samples, the Dubinin-Astakhov (DA) method was used to calculate the surface area from CO_2 isotherms at 273 K (Dubinin, 1975).

Adsorption Isotherms and Calculated Isothermic Heat of Adsorption of CO_2

CO_2 was purchased from Abelló-Linde with 99.9993% purity. Adsorption isotherms of CO_2 at temperatures ranging from 0 to 60°C were recorded up to 1 bar using a volumetric Micromeritics ASAP2010 and at higher pressures using a Hiden IGA3. The measured isotherms could be successfully fitted by either Virial, Toth, or Dual Site Langmuir models, which were used in the calculation of the isothermic heat of adsorption.

The procedure for the calculation of the isothermic heat of adsorption departs from the isotherms measured at 3 or more different temperatures. These isotherms are fitted to different isotherm models and the best fit is used for selecting pressure (P) values at constant loadings (Q) and different temperatures (T). Linear interpolation is also a valid way of doing this. The isothermic heat of adsorption (q_{st}) at each Q is then calculated, following Clausius-Clapeyrons' equation (Equation 1).

$$q_{st} = -R \left[\frac{\partial \ln P}{\partial \frac{1}{T}} \right]_Q \quad (1)$$

Where R is the ideal gas constant.

Estimated Framework Negative Charge

The estimated framework negative charge is a parameter that we have defined in order to be able to compare the isothermic heats of adsorption of materials with different chemical composition and connectivities. In the case of zeolites, it equals the $\text{Al}/(\text{Si} + \text{Al})$ molar ratio calculated from the ICP-OES results. In the case of SAPOs, the estimated framework negative charge is calculated by combining the ICP-OES with the ^{29}Si MAS NMR analyses results. The $\text{Si}/(\text{Si} + \text{Al} + \text{P})$ ratio is obtained from the ICP-OES data, and it gives the Si fraction out of the tetrahedral framework atoms. However, due to the different possible substitution patterns of Si in SAPOs (as single or isolated Si atoms or as Si-rich domains or SiO_2 -islands), not all the Si atoms contribute equally to the framework charge. More specifically, isolated Si atoms contribute with 1 negative charge per substituted P atom, whilst the contribution of a Si-rich domain is proportionally smaller and depends on its size. In order to differentiate between both types of Si in SAPOs, we have fitted the ^{29}Si NMR spectra using two Gaussian functions centered at values between -100 and -120 ppm for SiO_2 -islands and at ca. -90 ppm, for isolated Si species. The Gaussian functions are integrated and the fraction of isolated Si is calculated. This fraction is multiplied times the $\text{Si}/(\text{Si} + \text{Al} + \text{P})$ ratio obtained from the ICP-OES data and the result is taken as the estimated framework negative charge. The minor contribution of the Si-islands was disregarded. The estimated framework negative charge of AlPOs and pure-silica zeolites is taken as zero.

RESULTS

Characterization

XRD analysis confirmed the structural purity and degree of crystallinity of all of the calcined and/or dry materials (see **Supplementary Figure 3**).

Compositional analysis using ICP was used to determine the content of Al, Si, and P in all the samples (**Table 1**).

Solid State NMR analysis of ^{27}Al , ^{29}Si , and ^{31}P was used in order to study the local environments of the different framework atoms. All the recorded spectra can be found in **Supplementary Figures 4–6**. Aluminum was found with tetrahedral coordination (50–30 ppm) but also pentacoordinated (25–10 ppm) and octahedral (0 to –20 ppm) in AlPOs and SAPOs after calcination. In addition, several signals are observed in the ^{31}P spectra of AlPOs and SAPOs. These observations are primarily due to hydration of the framework, however hydration issues lay outside of the scope of this work. The ^{29}Si NMR analysis allowed us to determine how much of the Si could be found as SiO_2 -islands (–105 to –120 ppm), and how much of it was isolated, i.e., surrounded by 4 Al (–80 to –100 ppm).

The estimated framework negative charge was obtained as described in section Estimated Framework Negative Charge for the different materials and the values obtained are listed on **Table 1**. The results are discussed along with the isosteric heats of adsorption in section Isosteric Heats of Adsorption of CO_2 .

Nitrogen adsorption at 77K was used in most samples to obtain their BET surface area applying Rouquerol's criterion and the micropore volumes using the t-plot method. However, in some zeolites with high Al content (and thus, smaller pores due to the presence of extraframework cations), nitrogen could not enter the porosity in these conditions. In those samples the surface area was calculated from the isotherm of CO_2 at 273 K following Dubinin-Astakhov's (DA) method. In some samples,

especially when the CO_2 isotherm was close to saturation, both values were obtainable and are well-comparable. The results are presented in **Table 2**. It can be seen that for materials with the same structure, the calculated BET surface area and the t-plot micropore volume values are very similar. The DA surface area, however, presents larger differences between isostructural samples. In the case of LTA-4.5 ($680 \text{ m}^2 \text{ g}^{-1}$) and LTA-3 ($609 \text{ m}^2 \text{ g}^{-1}$) the reason may be the different available Na-sites for adsorption and their specific interaction with CO_2 . In the case of CHA-6 ($600 \text{ m}^2 \text{ g}^{-1}$) and CHA-3 ($470 \text{ m}^2 \text{ g}^{-1}$) the difference is remarkable and, although the interactions with some adsorption sites (Na and K ions, respectively) may be different, the presence of potassium itself reduces the average pore size thus diminishing the accessible area for CO_2 and any other adsorbate. In fact in the CHA-3 sample, N_2 could not enter the pores at 77 K.

CO_2 Isotherms

The recorded CO_2 isotherms at 25°C and up to 1 bar are presented in **Figures 1A–F**. Isotherms at different temperatures can be found in the SM. A general trend that we observe is that the higher the framework charge (proportional to the Al content in zeolites and to the amount of isolated Si in SAPOs), the steeper the low pressure regime of the isotherm. This is already an indicative of what we will find when comparing the adsorption heats. Moreover, the adsorption isotherms of AlPOs and SAPOs are similar to those of high Si/Al zeolites and reach saturation at much higher pressures (above 5 bar) than low Si/Al zeolites (above 1 bar). The maximum loading at saturation that can be estimated from the isotherms on LTA and CHA materials is comparable in all materials with the same structure and in both cases around 5 mmol/g .

Isosteric Heats of Adsorption of CO_2

The isosteric heat of adsorption of all materials was calculated at different loading values (Q) using the linear interpolation method for the sake of comparability, as the best isotherm fit differed from case to case. The results are plotted in **Figures 2A–F**. An initial drop of the q_{st} with Q is seen in most AlPO and SAPO materials, and it is related to energetic inhomogeneities on the adsorbent surface. After reaching a minimum value, the q_{st} rises slowly with loading, this meaning that the lateral interactions between CO_2 molecules are stronger than the adsorbate-adsorbent interactions (Sircar and Myers, 2003). Zeolites with high Al contents tend to present just the opposite behavior. It is noteworthy that all the q_{st} trends at high loading approach slowly values between 25 and 30 kJ/mol , which are close to the sublimation enthalpy of CO_2 . This indicates that at high loadings, the lateral interactions between CO_2 molecules may resemble those that can be found in solid CO_2 (U.S. Secretary of Commerce).

AlPO-42 and SAPO-42-104 present very similar isotherms and heats of adsorption (see **Figure 2A**), which is logical if we take into account that most of the Si in SAPO-42-104 is present as Si-islands, i.e., as “pure silica domains.” SAPO-42-13 and SAPO-42-24, both of which have predominantly isolated Si, the first having more than double the amount of Si in its framework, present a similar q_{st} starting value but for SAPO-42-24, there is a rapid decrease of the q_{st} to a value ca. 3 kJ/mol lower

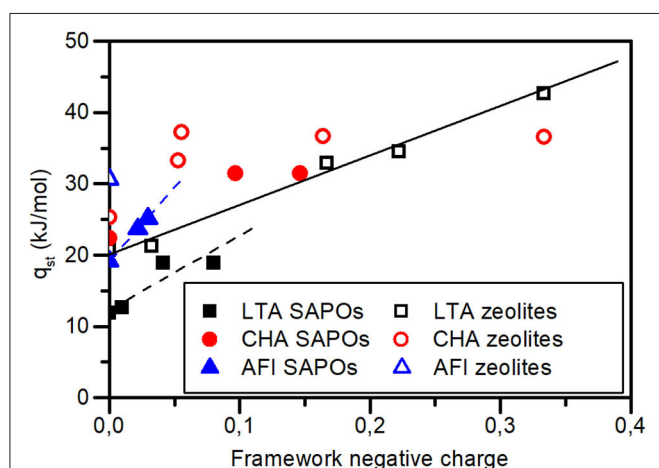


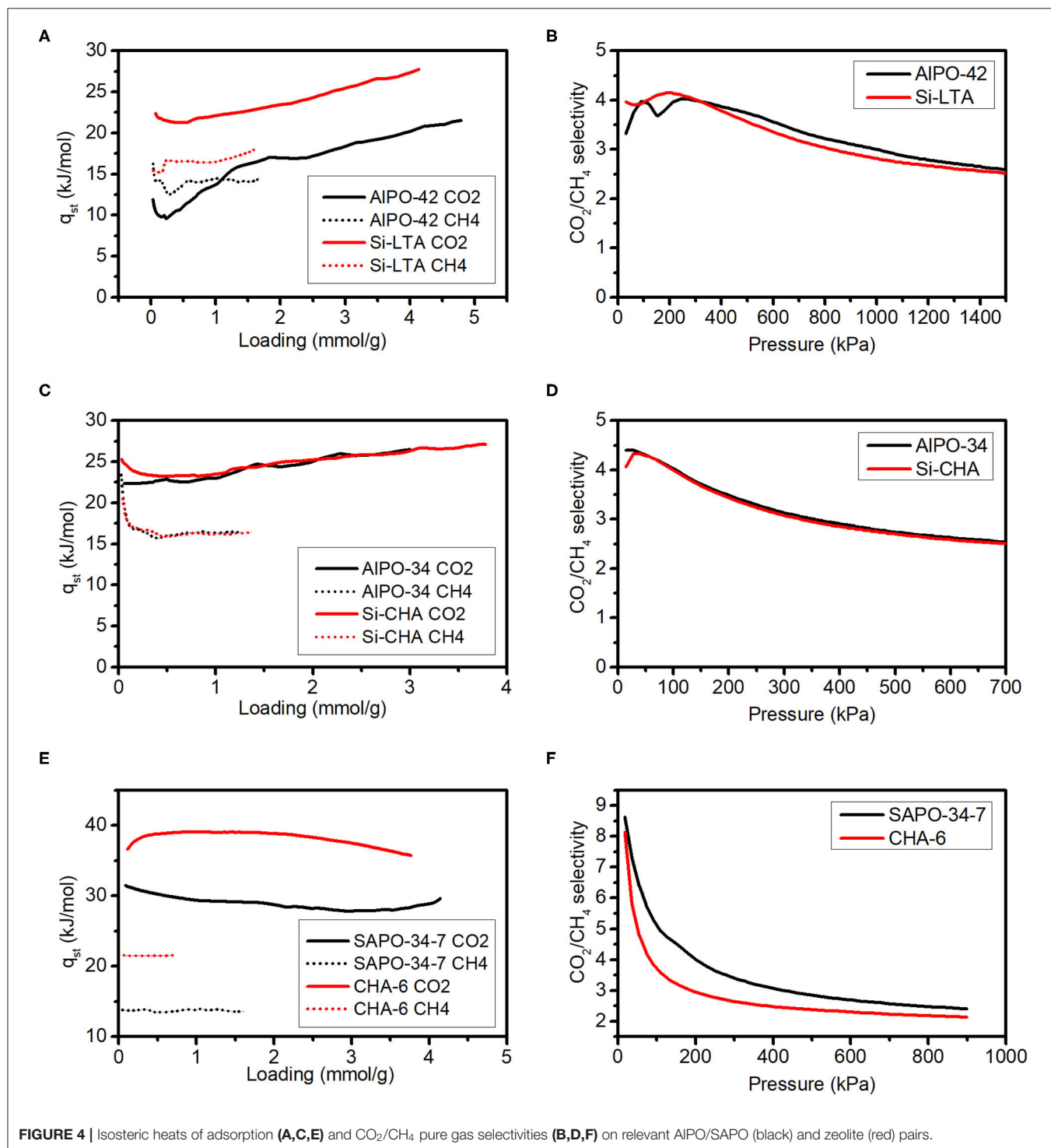
FIGURE 3 | Isosteric heats of adsorption on zeolites (open symbols), AlPOs and SAPOs (filled symbols) of LTA (black squares), CHA (red circles), and AFI (blue triangles) structures at low CO_2 loadings plotted against the estimated negative framework charge. The points labeled as SAPOs that fall in the vertical axis (zero framework charge) correspond to AlPOs.

(see **Figure 2A**). The q_{st} of zeolites with this structure is in all cases well above that of SAPO and AIPO materials and follows the expected trend.

The q_{st} on AIPO-34 is a bit lower than on its pure silica counterpart at low loadings but they follow a very similar trend at loadings above 0.5 mmol/g (see **Figure 2C**). Materials SAPO-34-10 and SAPO-34-7 (see **Figure 2C**), together with

zeolites CHA-19 and CHA-18 (see **Figure 2D**) present q_{st} trends that descend initially and are in the range 25–35 kJ/mol. Zeolites CHA-6 and CHA-3, with the highest Al contents, present q_{st} values above 35 kJ/mol, that initially increase (see **Figure 2D**).

All materials with AFI structure present an initial decrease of the q_{st} , with the AIPO-5 having the lowest values, notably below the SAPOs and Si-AFI (see **Figures 2E,F**). SAPO-5-46 has a lower



q_{st} than SAPO-5-34 in the whole range (see **Figure 2E**), as would be expected from their respective framework charges.

The mentioned general trend of SAPOs and AIPOs is interesting for their application as CO₂ adsorbents, not only because of their generally low q_{st} values, which will result in an easy regeneration of the adsorbent, but also because of the increase of q_{st} with loading above 1 mmol/g. This means that desorbing will be progressively easier until the minimum in q_{st} is reached.

The isosteric heats of adsorption at the lowest loadings possible have been plotted against the estimated framework negative charge (see **Figure 3**, Palomino's Plot), as was done previously for LTA zeolites (Palomino et al., 2010). This shows that AIPOs and SAPOs with AFI and LTA structures also present the same linear relation (discontinuous straight lines, **Figure 3**) seen previously in LTA zeolites (continuous straight line, **Figure 3**) and that these materials present notably lower heats of CO₂ adsorption than their zeolitic counterparts, even the pure silica analogs. This is striking, as the studied pure silica zeolite samples do not present a significant amount of connectivity defects (**Supplementary Figure 7**) and they are usually regarded as quite inert materials. In the case of materials with CHA structure, there is also an increase of the q_{st} at low loading with increasing framework negative charge, but we cannot affirm that it is a linear relationship. On the other hand, the q_{st} of CHA zeolites seems to be higher than that of SAPOs and AIPOs with the same framework negative charge, but the trend is less clear than for the other structures.

Comparison of AIPOs/SAPOs and Zeolites in Terms of CO₂ and CH₄ Adsorption

As examples of the advantages that AIPOs and SAPOs can have over zeolites in the field of CO₂ adsorption and separation, we establish here several relevant comparisons between materials included in this study in terms of their CO₂/CH₄ separation ability (**Figure 4** and **Table 3**). Materials that have been compared have the same structure and equal (or similar) estimated framework charge values, and are activated prior to adsorption at 400°C and under vacuum, which means that the differences in adsorption and selectivity will only stem from differences in the relative interactions of the adsorbates with the framework. The selectivities presented in **Figure 4** have been calculated from the pure component isotherms as the ratio of adsorbed amounts at each pressure value. The CO₂ ideal working capacities for a pressure swing adsorption (PSA) process shown in **Table 3** have been calculated by subtracting the maximum loadings at 5 and 1 bar. This is an oversimplification, as in a PSA process the adsorbent will be in contact with a mixture and the adsorption of a component will be different from the pure state, but it is a useful approach to first compare different adsorbents (Bacsik et al., 2016).

As can be seen from **Figure 4A**, the q_{st} of both CO₂ and CH₄ are lower on AIPO-42 compared to Si-LTA. The selectivity calculated as the ratio of the isotherms of the pure gases is very similar between AIPO-42 and Si-LTA (**Figure 4B**). Their working capacities are quite similar, with the AIPO-42 being slightly above

TABLE 3 | Carbon dioxide loadings at 1 and 5 bar of some adsorbents and their PSA working capacity.

	Q _{1bar} (mmol/g)	Q _{5bar} (mmol/g)	Working capacity (mmol/g)
AIPO-42	1.26	4.47	3.21
Si-LTA	1.18	4.17	2.99
AIPO-34	1.6	3.5	1.9
Si-CHA	2.24	4.62	2.38
SAPO-34-7	2.8	4.64	1.84
CHA-6	4.65	5.66	1.01

ITQ-29. In the case of AIPO-34 and Si-CHA, the both materials are identical in terms of CH₄ q_{st} and pure gas selectivities (**Figures 4C,D**), although the CO₂ q_{st} at low loadings is lower for AIPO-34. However, the Si-CHA presents a notably higher CO₂ adsorption capacity and also a higher working capacity. If we go to a more complex case, and compare SAPO-34-7 material with aluminosilicate zeolite CHA-6, both presenting an estimated framework charge close to 0.15, the differences in the q_{st} of both CH₄ and CO₂ are large and the selectivity in SAPO-34-7 is above that of CHA-6. Furthermore, going from the zeolite to the SAPO material in this case also implies a large decrease in the adsorption capacity at 1 bar, which in turn translates into a much larger working capacity of the SAPO-34-7.

With these three examples, we point out the fact that by using AIPO/SAPO adsorbents instead of zeolites, the separation of carbon dioxide from methane can be done keeping very similar maximum capacities and selectivities whilst also lowering the energy needed for regeneration.

CONCLUSIONS

In this work we have identified a general trend according to which the isosteric heat of adsorption of CO₂ on AIPOs and SAPOs with AFI, LTA and CHA structures is lower than on the isostructural zeolites, even of pure silica composition. This decrease in q_{st} when going from zeolites to AIPOs and SAPOs is not accompanied by a decrease in CO₂/CH₄ selectivity, as can be seen for materials with LTA and CHA structure. These facts lead to believe that if implemented in a CO₂ capture process, AIPOs and SAPOs can lower the energy needed for regeneration of the adsorption bed whilst keeping the efficiency of the separation.

DATA AVAILABILITY STATEMENT

All datasets presented in this study are included in the article/**Supplementary Material**.

AUTHOR CONTRIBUTIONS

EP-B participated in the synthesis of the AFI materials and AIPO-42, performed part of the adsorption experiments, analyzed the characterization results and the adsorption data to obtain the isosteric heats of adsorption, coordinated the work of his colleagues, and wrote the main part of this work. RM-F

performed the synthesis of the SAPO-42 materials and analyzed their Si-distribution. NG-C performed the synthesis of the AlPO-34 material. AC together with NG-C synthesized the template of the AlPO-34 material. MP performed part of the adsorption experiments and the analysis of these to obtain the isosteric heats of adsorption. MM supervised the synthesis and characterization of SAPO-42 and SAPO-34 materials, and analyzed their Si-distribution. SV supervised the synthesis and characterization of materials. FR supervised the characterization of the materials and the data analysis and coordinated the work of the whole team. All authors contributed to the article and approved the submitted version.

FUNDING

We acknowledge the Spanish Ministry of Sciences, Innovation and Universities (MCIU), State Research Agency (AEI), and the European Fund for Regional Development (FEDER) for their funding via projects Multi2HYcat (EU-Horizon 2020 funded project under grant agreement no. 720783),

Program Severo Ochoa SEV-2016-0683 and RTI2018-101033-B-I00 and also Fundación Ramón Areces for funding through a research contract (CIVP18A3908). EP-B thanks the MCIU for his grant (FPU15/01602). NG-C thanks MCIU for her grant (BES-2016-078178).

ACKNOWLEDGMENTS

The authors want to thank Alejandro Vidal Moya for his help analyzing the NMR results. We also thank Jose Luis Jorda for carrying out the high temperature XRD experiments. Also special thanks to Jose Valero, Isabel Millet, and Amparo Moraleda for synthesizing most of the materials used in this work. The Electron Microscopy Service of the UPV is acknowledged.

SUPPLEMENTARY MATERIAL

The Supplementary Material for this article can be found online at: <https://www.frontiersin.org/articles/10.3389/fchem.2020.588712/full#supplementary-material>

REFERENCES

- Bacsik, Z., Cheung, O., Vasiliev, P., and Hedin, N. (2016). Selective separation of CO₂ and CH₄ for biogas upgrading on zeolite NaKA and SAPO-56. *Appl. Energy* 162, 613–621. doi: 10.1016/j.apenergy.2015.10.109
- Baerlocher, C. H., and McCusker, L. B. *Database of Zeolite Structures*. Available online at: <http://www.iza-structure.org/databases/> (accessed July 17, 2020).
- Boot-Handford, M. E., Abanades, J. C., Anthony, E. J., Blunt, M. J., Brandani, S., Mac Dowell, N., et al. (2014). Carbon capture and storage update. *Energy Environ. Sci.* 7, 130–189. doi: 10.1039/C3EE42350F
- Bourgogne, M., Guth, J.-L., and Wey, R. (1985). *Process for the Preparation of Synthetic Zeolites, and Zeolites Obtained by Said Process*. Available online at: <https://patents.google.com/patent/US4503024A/en>.
- Bui, M., Adjiman, C. S., Bardow, A., Anthony, E. J., Boston, A., Brown, S., et al. (2018). Carbon capture and storage (CCS): the way forward. *Energy Environ. Sci.* 11, 1062–1176. doi: 10.1039/C7EE02342A
- Cheung, O., Liu, Q., Bacsik, Z., and Hedin, N. (2012). Silicoaluminophosphates as CO₂ sorbents. *Microporous Mesoporous Mater.* 156, 90–96. doi: 10.1016/j.micromeso.2012.02.003
- Corma, A., Rey, F., Rius, J., Sabater, M. J., and Valencia, S. (2004). Supramolecular self-assembled molecules as organic directing agent for synthesis of zeolites. *Nature* 431, 287–290. doi: 10.1038/nature02909
- Dawson, D. M., Griffin, J. M., Seymour, V. R., Wheatley, P. S., Amri, M., Kurkiewicz, T., et al. (2017). A multinuclear NMR study of six forms of AlPO-34: structure and motional broadening. *J. Phys. Chem. C* 121, 1781–1793. doi: 10.1021/acs.jpcc.6b11908
- Díaz-Cabañas, M.-J., and Barrett, P. A. (1998). Synthesis and structure of pure SiO₂ chabazite: the SiO₂ polymorph with the lowest framework density. *Chem. Commun.* 29, 1881–1882. doi: 10.1039/a804800b
- Dubinin, M. M. (1975). “Physical adsorption of gases and vapors in micropores,” in *Progress in Surface and Membrane Science*, eds D. A. Cadenhead, J. F. Danielli, and M. D. Rosenberg (New York, NY: Elsevier), 1–70. doi: 10.1016/B978-0-12-571809-7.50006-1
- Fischer, M. (2017). Computational evaluation of aluminophosphate zeotypes for CO₂/N₂ separation. *Phys. Chem. Chem. Phys.* 19, 22801–22812. doi: 10.1039/C7CP03841K
- García, E. J., Pérez-Pellitero, J., Pirngruber, G. D., Jallut, C., Palomino, M., Rey, F., et al. (2014). Tuning the adsorption properties of zeolites as adsorbents for CO₂ separation: best compromise between the working capacity and selectivity. *Ind. Eng. Chem. Res.* 53, 9860–9874. doi: 10.1021/ie500207s
- Girnus, I., Jancke, K., Vetter, R., Richter-Mendau, J., and Caro, J. (1995). Large AlPO₄-5 crystals by microwave heating. *Zeolites* 15, 33–39. doi: 10.1016/0144-2449(94)00004-C
- Global CCS Institute (2019). *Global Status Report of CCS*. Available online at: https://www.globalccsinstitute.com/wp-content/uploads/2019/12/GCC_GLOBAL_STATUS_REPORT_2019.pdf.
- IZA. *International Zeolite Association Synthesis Commission*. Available online at: <http://www.iza-online.org/synthesis/default.htm> (accessed June 1, 2020).
- Küehl, G. H. (1980). *Preparation of Shape Selective Zeolite Alpha as Catalyst*. US Patent 4191663 A.
- Lee, K. B., Beaver, M. G., Caram, H. S., and Sircar, S. (2008). Reversible chemisorbents for carbon dioxide and their potential applications. *Ind. Eng. Chem. Res.* 47, 8048–8062. doi: 10.1021/ie800795y
- Lee, S. Y., and Park, S. J. (2015). A review on solid adsorbents for carbon dioxide capture. *J. Ind. Eng. Chem.* 23, 1–11. doi: 10.1016/j.jiec.2014.09.001
- Lemishko, T., Valencia, S., Rey, F., Jiménez-Ruiz, M., and Sastre, G. (2016). Inelastic neutron scattering study on the location of bronsted acid sites in high silica LTA zeolite. *J. Phys. Chem. C* 120, 24904–24909. doi: 10.1021/acs.jpcc.6b09012
- Leung, D. Y. C., Caramanna, G., and Maroto-Valer, M. M. (2014). An overview of current status of carbon dioxide capture and storage technologies. *Renew. Sustain. Energy Rev.* 39, 426–443. doi: 10.1016/j.rser.2014.07.093
- Liu, X., Vlugt, T. J. H., and Bardow, A. (2011). Maxwell-Stefan diffusivities in liquid mixtures: using molecular dynamics for testing model predictions. *Fluid Phase Equilib.* 301, 110–117. doi: 10.1016/j.fluid.2010.11.019
- Lok, B. M., Messina, C. A., Patton, R. L., Gajek, R. T., Cannan, T. R., and Flanigen, E. M. (1984). *Crystalline Silicoaluminophosphates*. US Patent 4440871.
- Man, P. P., Briend, M., Peltre, M. J., Lamy, A., Beaunier, P., and Barthomeuf, D. (1991). A topological model for the silicon incorporation in SAPO-37 molecular sieves: correlations with acidity and catalysis. *Zeolites* 11, 563–572. doi: 10.1016/S0144-2449(05)80006-5
- Martin, C., Tosi-Pellenq, N., Patarin, J., and Coulomb, J. P. (1998). Sorption properties of AlPO₄-5 and SAPO-5 zeolite-like materials. *Langmuir* 14, 1774–1778. doi: 10.1021/la960755c
- Martínez-Franco, R., Cantín, Á., Vidal-Moya, A., Moliner, M., and Corma, A. (2015). Self-assembled aromatic molecules as efficient organic structure directing agents to synthesize the silicoaluminophosphate SAPO-42 with isolated Si species. *Chem. Mater.* 27, 2981–2989. doi: 10.1021/acs.chemmater.5b00337

- Martínez-Franco, R., Li, Z., Martínez-Triguero, J., Moliner, M., and Corma, A. (2016). Improving the catalytic performance of SAPO-18 for the methanol-to-olefins (MTO) reaction by controlling the Si distribution and crystal size. *Catal. Sci. Technol.* 6, 2796–2806. doi: 10.1039/C5CY02298C
- Miyamoto, M., Fujioka, Y., and Yogo, K. (2012). Pure silica CHA type zeolite for CO₂ separation using pressure swing adsorption at high pressure. *J. Mater. Chem.* 22, 20186. doi: 10.1039/c2jm34597h
- Moscoco, J. G., Lewis, G. J., Gisselquist, J. L., Miller, M. A., and Rohde, L. M. (2003). *Crystalline Aluminosilicate Zeolitic Composition: UZM-9*. WO 03068679 A1.
- Nordstrand, R. A., van Santilli, D. S., and Zones, S. I. (1988). “An all-silica molecular sieve that is isostructural with AlPO-5,” in *Perspectives in Molecular Sieve Science*, eds W. H. Flank and T. E. Whyte (Washington, DC: American Chemical Society), 236–245. doi: 10.1021/bk-1988-0368.ch015
- Palomino, M., Corma, A., Rey, F., and Valencia, S. (2010). New insights on CO₂-methane separation using LTA zeolites with different Si/Al ratios and a first comparison with MOFs. *Langmuir* 26, 1910–1917. doi: 10.1021/la9026656
- Pham, T. D., Hudson, M. R., Brown, C. M., and Lobo, R. F. (2014). Molecular basis for the high CO₂ adsorption capacity of chabazite zeolites. *ChemSusChem* 7, 3031–3038. doi: 10.1002/cssc.201402555
- Prakash, A. M., and Unnikrishnan, S. (1994). Synthesis of SAPO-34: high silicon incorporation in the presence of morpholine as template. *J. Chem. Soc. Faraday Trans.* 90, 2291–2296. doi: 10.1039/ft9949002291
- Riboldi, L., and Bolland, O. (2017). Overview on pressure swing adsorption (PSA) as CO₂ capture technology: state-of-the-art, limits and potentials. *Energy Procedia* 114, 2390–2400. doi: 10.1016/j.egypro.2017.03.1385
- Rubin, E. S., Davison, J. E., and Herzog, H. J. (2015). The cost of CO₂ capture and storage. *Int. J. Greenh. Gas Control* 40, 378–400. doi: 10.1016/j.ijggc.2015.05.018
- Schreyeck, L., Stumbe, J., Caultet, P., Mougénel, J.-C., and Marler, B. (1998). The diaza-polyoxa-macrocyclic “Kryptofix222” as a new template for the synthesis of LTA-type AlPO₄. *Microporous Mesoporous Mater.* 22, 87–106. doi: 10.1016/S1387-1811(98)00082-1
- Shang, J., Li, G., Singh, R., Gu, Q., Nairn, K. M., Bastow, T. J., et al. (2012). Discriminative separation of gases by a “molecular trapdoor” mechanism in chabazite zeolites. *J. Am. Chem. Soc.* 134, 19246–19253. doi: 10.1021/ja309274y
- Sircar, S., and Myers, A. (2003). “Gas separation by zeolites,” in *Handbook of Zeolite Science and Technology*, eds S. M. Auerbach, K. A. Carrado, and P. K. Dutta (New York-Basel: Marcel-Dekker), 1062–1103. doi: 10.1201/9780203911167.ch22
- Tagliabue, M., Farrusseng, D., Valencia, S., Aguado, S., Ravon, U., Rizzo, C., et al. (2009). Natural gas treating by selective adsorption: material science and chemical engineering interplay. *Chem. Eng. J.* 155, 553–566. doi: 10.1016/j.cej.2009.09.010
- The National Academies of Sciences, Engineering and Medicine (2018). *Negative Emissions Technologies and Reliable Sequestration: A Research Agenda*. Washington, DC: The National Academies Press.
- Thommes, M., Kaneko, K., Neimark, A. V., Olivier, J. P., Rodriguez-Reinoso, F., Rouquerol, J., et al. (2015). Physisorption of gases, with special reference to the evaluation of surface area and pore size distribution (IUPAC Technical Report). *Pure Appl. Chem.* 87, 1051–1069. doi: 10.1515/pac-2014-1117
- U.S. National Coal Council (2015). *Fossil Forward: Revitalizing CCS*. Washington, DC: U.S. National Coal Council.
- U.S. Secretary of Commerce. *NIST Chemistry WebBook, SRD 69—Carbon Dioxide*. Available online at: <https://webbook.nist.gov/cgi/cbook.cgi?ID=C124389&Mask=4#Thermo-Phase> (accessed June 1, 2020).
- Wilson, S. T., Lok, B. M., Messina, C. A., Cannan, T. R., and Flanigen, E. M. (1982). Aluminophosphate molecular sieves: a new class of microporous crystalline inorganic solids. *J. Am. Chem. Soc.* 104, 1146–1147. doi: 10.1021/ja00368a062
- Wright, P. A., and Connor, J. A. (2008). “Families of microporous framework solids,” in *Microporous Framework Solids RSC Materials Monographs* (Cambridge: Royal Society of Chemistry), 8–78.
- Young, D., and Davis, M. E. (1991). Studies on SAPO-5: synthesis with higher silicon contents. *Zeolites* 11, 277–281. doi: 10.1016/S0144-2449(05)80232-5
- Zibrowius, B., Löfler, E., and Hunger, M. (1992). Multinuclear MAS NMR and IR spectroscopic study of silicon incorporation into SAPO-5, SAPO-31, and SAPO-34 molecular sieves. *Zeolites* 12, 167–174. doi: 10.1016/0144-2449(92)90079-5
- Zones, S. I. (1991). Conversion of faujasites to high-silica chabazite SSZ-13 in the presence of *N, N, N*-trimethyl-1-adamantammonium iodide. *J. Chem. Soc. Faraday Trans.* 87:3709. doi: 10.1039/ft9918703709
- Zones, S. I., and van Nordstrand, R. A. (1988). Novel zeolite transformations: the template-mediated conversion of cubic P zeolite to SSZ-13. *Zeolites* 8, 166–174. doi: 10.1016/S0144-2449(88)80302-6

Conflict of Interest: The authors declare that the research was conducted in the absence of any commercial or financial relationships that could be construed as a potential conflict of interest.

Copyright © 2020 Pérez-Botella, Martínez-Franco, González-Camuñas, Cantín, Palomino, Moliner, Valencia and Rey. This is an open-access article distributed under the terms of the Creative Commons Attribution License (CC BY). The use, distribution or reproduction in other forums is permitted, provided the original author(s) and the copyright owner(s) are credited and that the original publication in this journal is cited, in accordance with accepted academic practice. No use, distribution or reproduction is permitted which does not comply with these terms.